**Electronic Supplementary Information (ESI)**

# High-performance Bi-functional Electrocatalysts of 3D Crumpled Graphene-Cobalt Oxide Nanohybrids for Oxygen Reduction and Evolution Reactions

**Shun Mao[1], Zhenhai Wen[1], Taizhong Huang[1,2], Yang Hou[1], and Junhong Chen[1]***

[1]Department of Mechanical Engineering, University of Wisconsin-Milwaukee, 3200 N Cramer Street, Milwaukee, WI 53211, USA.
[2]Key Laboratory of Chemical Sensing & Analysis in Universities of Shandong, School of Chemistry and Chemical Engineering, University of Jinan, Jinan, 250022, China.

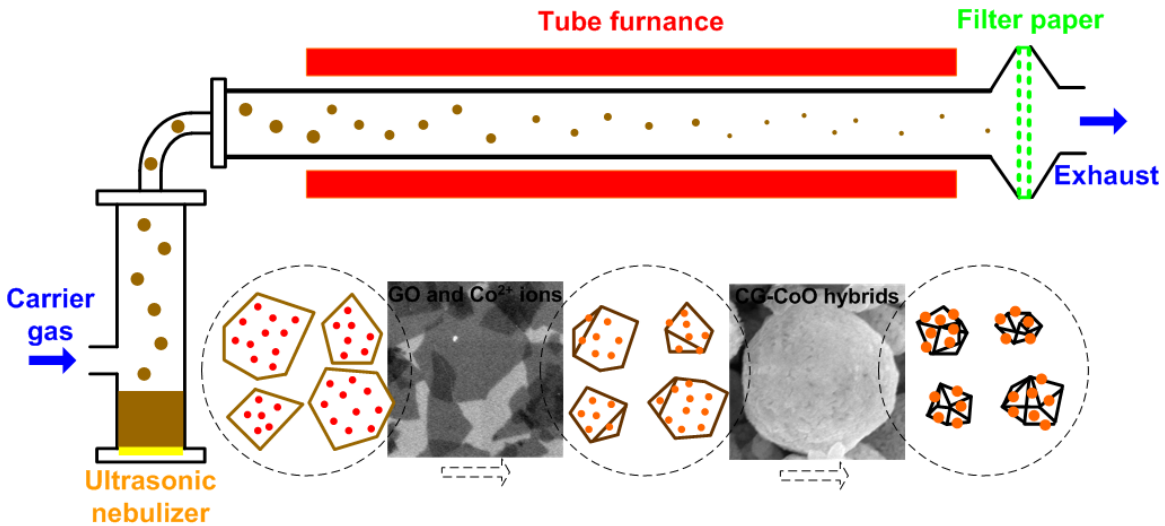


**Fig. S1** Preparation of CG-nanocrystal hybrids by rapid compression of GO sheets in evaporating aerosol droplets and simultaneous chemical reactions for growth of nanocrystals on the CG surface. Schematic illustration of the experimental setup and the aerosolization/high temperature-induced GO crumpling and CoO nanocrystal growth process. The CG-CoO hybrids were collected with a filter paper at the downstream of the tube furnace.

## Electrochemical Measurements

### 1. RHE conversion

A saturated silver chloride electrode was used as the reference electrode in all measurements. The measured potentials versus the Ag/AgCl reference electrode were converted to the reversible hydrogen electrode (RHE) scale via the Nernst equation:

$$E_{RHE} = E_{Ag/AgCl} + 0.059\,pH + E^{o}{}_{Ag/AgCl} \quad (1)$$

where $E_{RHE}$ is the converted potential versus RHE, $E_{Ag/AgCl}$ is the experimental potential measured against the Ag/AgCl reference electrode, and $E^{o}{}_{Ag/AgCl}$ is the standard potential of Ag/AgCl at 25 °C (0.1976 V). The electrochemical measurements were carried out in 1 M KOH (pH = 14) at room temperature; therefore, $E_{RHE} = E_{Ag/AgCl} + 1.024$ V.

### 2. Rotating disk electrode (RDE) measurement

The rotating disk electrode (RDE) measurement was carried out to study the kinetics of electrochemical catalytic ORR of the prepared catalyst. The polarization curves with different rotation rates (Fig. 3) and their corresponding Koutecky-Levich plots with the inverse current density ($J^{-1}$) versus the inverse of the square root of the rotation speed ($\omega^{-1/2}$) at different potentials are given. The slopes of their best linear fit lines were used to calculate the electron transfer number ($n$) based on the Koutecky-Levich equation:

$$\frac{1}{J} = \frac{1}{J_L} + \frac{1}{J_K} = \frac{1}{B\omega^{1/2}} + \frac{1}{J_K} \quad (2)$$

$$B = 0.62nFC_o(D_o)^{2/3}\nu^{-1/6} \quad (3)$$

$$J_K = nFkC_o \quad (4)$$

where $J$ is the measured current density, $J_K$ and $J_L$ are the kinetic- and diffusion- limiting current densities, $\omega$ is the angular velocity, $n$ is transferred electron number, F is the Faraday constant (96,485 $C \cdot mol^{-1}$), $C_o$ is the saturated concentration of $O_2$ in 1 M KOH at room temperature ($0.93\times10^{-6}$ $mol \cdot cm^{-3}$), $D_o$ is diffusion coefficient of oxygen in water ($1.30\times10^{-5}$ $cm^2 \cdot s^{-1}$), $\upsilon$ is kinematic viscosity of the electrolyte at room temperature ($5.45\times10^{-3}$ $cm^2 \cdot s^{-1}$), and $k$ is the electron-transfer rate constant. According to the Koutecky–Levich plot, the slope (1/B) can be used for calculating the electron transfer number, namely $n = B/(0.62FCoDo^{2/3}\upsilon^{-1/6})$. For the Tafel plot, the kinetic current was calculated from the mass-transport correction of RDE by:

$$J_k = \frac{(J \times J_L)}{(J_L - J)} \quad (5)$$

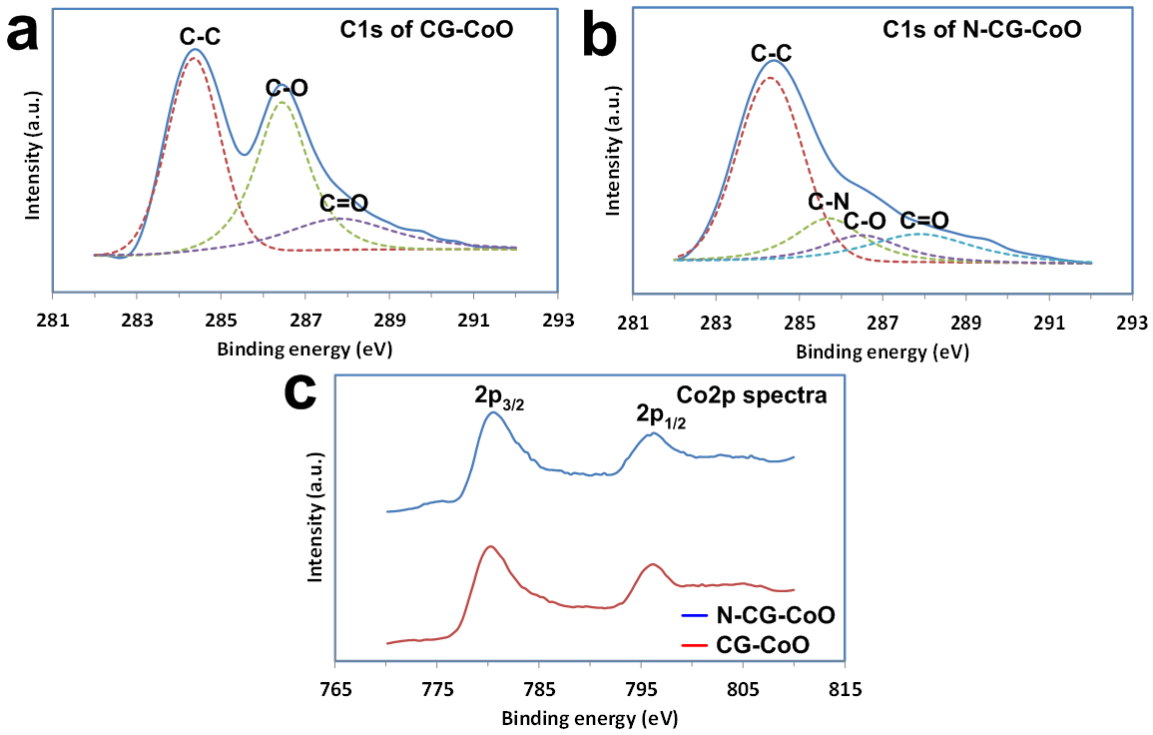


**Fig. S2** High-resolution C1s spectra and curve fits of (a) CG-CoO and (b) N-CG-CoO hybrids. (c) High-resolution Co2p spectra of N-CG-CoO and CG-CoO hybrids. From the C1s spectra of CG-CoO, three peaks centered at 284.4, 286.5, and 287.8 eV are observed, corresponding to C–C, C–O, and C=O groups, respectively. After thermal annealing in ammonia, the C-N peak located at 285.7 eV is evidenced, indicating that the nitrogen was doped into the carbon lattice of CG. It is also found that the intensities of C–O and C=O peaks greatly decreased, revealing that large amount of oxygen-containing groups were removed during the annealing and the CG was further reduced. The Co2p spectra of the N-CG-CoO and CG-CoO are very similar, indicating that there is no significant structure change in the CoO nanocrystal after thermal annealing in ammonia. The Co2p spectra further confirm that N dopants were in CG sheets but not in CoO nanocrystals.

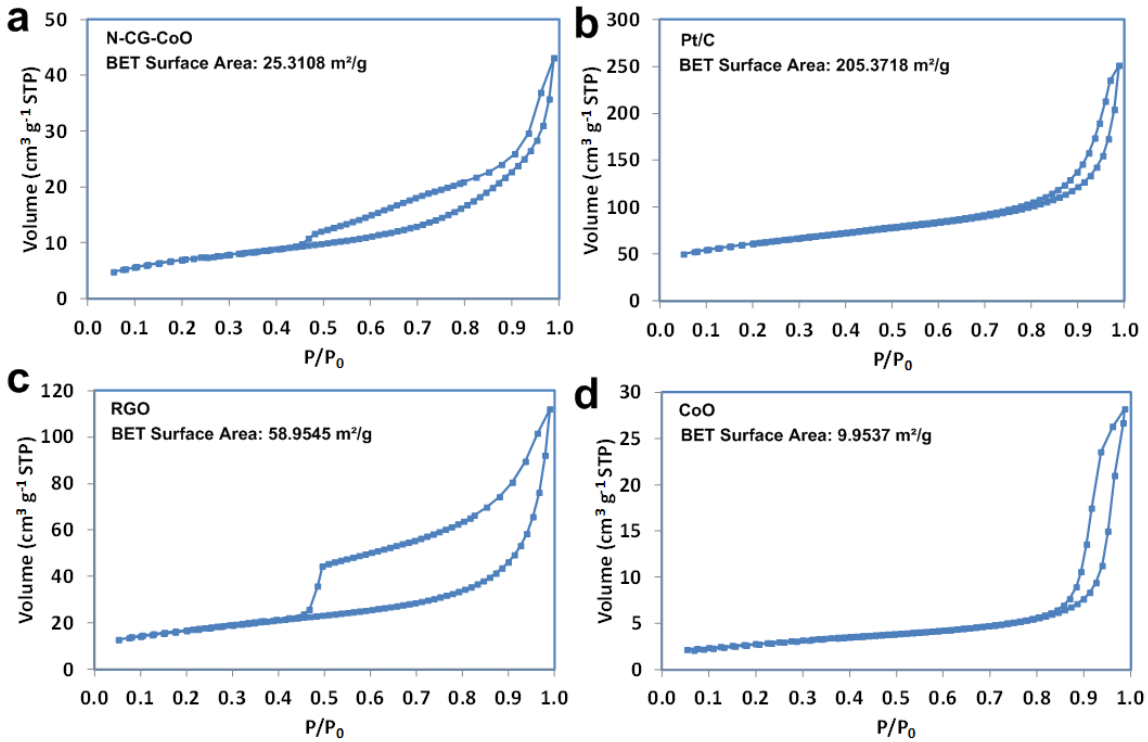


**Fig. S3** Nitrogen adsorption/desorption isotherms of (a) N-CG-CoO, (b) commercial Pt/C, (c) RGO, and (d) CoO. The nitrogen adsorption-desorption isotherm curves of N-CG-CoO show type IV isotherms with a distinct hysteresis loop at a relative pressure $P/P_0$ ranging from 0.45 to 1. The measured BET surface area of the N-CG-CoO is 25.31 $m^2 \cdot g^{-1}$; while the BET surface areas of commercial Pt/C, RGO, and CoO are 205.37, 58.95, and 9.95 $m^2 \cdot g^{-1}$, respectively. The N-CG-CoO catalyst has a smaller BET surface area but a higher catalytic activity than commercial Pt/C and RGO, suggesting that the N-CG-CoO catalyst has excellent catalytic performance in ORR.

**Table S1** Electrochemical parameters of ORR and OER bi-functional catalysts.

| Reaction | Parameters | N-CG-CoO | $H_2$-CoCat | $Co_3O_4$/N-rmGO | (GO 8 wt.%) Cu-MOF | $CaMn_4Ox$ |
|---|---|---|---|---|---|---|
| | | This work | Cobo et al. in *Nature Materials*[1] | Liang et al. in *Nature Materials*[2] | Jahan et al. in *Advanced Functional Materials*[3] | Gorlin et al. in *Journal of the American Chemical Society*[4] |
| ORR | Onset potential (V vs. RHE) | 0.90 | | 0.86 | 0.29 | 0.85 |
| | Tafel slope (mV/dec) | 48 | | 37 | 69 | |
| OER | Onset potential (V vs. RHE) | 1.30 | 1.775 for oxygen evolution | 1.35-1.40 | 1.19 | 1.20-1.30 |
| | Overpotential (V vs. RHE) at 10 $mA \cdot cm^{-2}$ | 0.34 | | 0.31 | 0.35-0.36 | 0.54 |
| | Tafel slope (mV/dec) | 71 | | 67 | 65 | |

Table. S1 summarizes key electrochemical parameters of some previously reported bi-functional catalysts for ORR and OER. From this table, it is clearly shown that the catalytic performance of our catalyst in ORR and OER are comparable and even better than some of the best catalysts ever reported, e.g., a high positive onset potential and small Tafel slope for ORR and a small overpotential at 10 $mA \cdot cm^{-2}$ for OER.

References:

1. S. Cobo, J. Heidkamp, P.-A. Jacques, J. Fize, V. Fourmond, L. Guetaz, B. Jousselme, V. Ivanova, H. Dau, S. Palacin, M. Fontecave and V. Artero, *Nat. Mater.*, 2012, **11**, 802.
2. Y. Liang, Y. Li, H. Wang, J. Zhou, J. Wang, T. Regier and H. Dai, *Nat. Mater.*, 2011, **10**, 780.
3. M. Jahan, Z. Liu and K. P. Loh, *Adv. Funct. Mater.*, 2013, n/a.
4. Y. Gorlin and T. F. Jaramillo, *J. Am. Chem. Soc.*, 2010, **132**, 13612.